Proceedings of Meetings on Acoustics

Volume 6, 2009 http://asa.aip.org

157th Meeting
Acoustical Society of America
Portland, Oregon
18 - 22 May 2009
Session 3aSA: Structural Acoustics and Vibration

3aSA7. Single Antenna Time Reversal of Guided Waves in Pipelines

Nicholas O'Donoughue*, Joel Harley, Jose M. Moura, Yuanwei Jin, Irving Oppenheim, Yujie Ying, Joseph States, James Garrett and Lucio Soibelman

***Corresponding author's address: Electrical & Computer Engineering, Carnegie Mellon University, PH B9 - ECE Dept, Pittsburgh, PA 15213, nodonoug@andrew.cmu.edu**

The volatile nature of natural gas makes it extremely important to ensure that distribution pipelines remain free from defects, as leakage can result in explosions. Many current methods for testing buried pipelines rely on periodic excavation of a section of pipe and attachment of large acoustic or magneto-restrictive sensors. These systems, while reliable, suffer from a high cost-per-test ratio. Our group hopes to reduce the power constraints of such a detection system, in order to allow for permanent installations that monitor the pipelines continuously. We propose to use Time Reversal, a signal processing technique, in order to achieve this improvement. This paper will focus on the modes generated by various acoustic probing signals, and the echoes received with and without Time Reversal. We argue that TR will be most beneficial when there are several dispersive modes present, a scenario avoided in conventional techniques. We will present simulation results for the analysis of wave modes in a cylindrical pipe before and after Time Reversal using PZFlex.

Published by the Acoustical Society of America through the American Institute of Physics

 [DOI: 10.1121/1.3155375]
Received 21 May 2009; published 8 Jun 2009

1. INTRODUCTION

The previous title of this paper was 'Detection of Structural Defects in Time Reversal', and the title was changed due to a decision to continue our study of detection methods before presenting results. Instead, this paper focuses on the actual time reversal stage, and analyzed the effects on wave modes generated and signals received. The author list has been expanded to include additional members of the research team.

Ultrasonic guided waves are used in many commercial nondestructive testing applications due to their long propagation distances, but often suffer from the need to excavate sections of buried pipelines in order to attach the sensory equipment. What we hope to achieve is a reduction in the power constraints, and the number of transducers required at each testing position. This will make a permanent solution, one which remains in a monitoring mode, as opposed to periodic tests, more feasible. We will accomplish this task by exploiting the benefits of Time Reversal, a signal processing technique first pioneered by M. Fink (Fink 1992).

The use of guided waves for non-destructive testing in pipes is complicated by the propagation environment, which contains wave modes with frequency-dependent speed. In order to alleviate effects, many conventional systems use large rings of transducers to selectively excite a single wave mode, and a narrow bandwidth to limit dispersive effects. We hope to use Time Reversal to compensate for the effects without the need for expensive and power-hungry hardware.

Time Reversal has been shown to compensate for both dispersiveness and the multi-modal environments found in thin plates, where lamb waves exist (Ing & Fink 1998; Prada & Fink 1998), resulting in a compression of the wave in both time and space, as well as an increase in the peak signal level. From (Ing & Fink 1998; Prada & Fink 1998; Moura & Jin 2007; Moura & Jin 2008; Jin & Moura 2009), we know that Time Reversal's focusing effects are most visibly seen in extremely dense channels, with discrete echoes generated from scattering objects. We theorize that the same effect will be experienced from the superposition of a large number of wave modes. Although we do not test that theory within this paper, we rely on the results of (Ing & Fink 1998) and their conclusion that dispersion is beneficial to Time Reversal. Thus, we plan to excite as many modes as possible, with as much dispersion as possible, in order to maximize the potential for TR processing gain. We should note that, while many systems operate in a pulse-echo mode, we are devising this system for a pitch-catch scenario.

The scope of this paper is to analyze what modes are present in a thin-walled pipe before and after Time Reversal processing, and to demonstrate the time compression and focusing effects of TR for pipes. These properties will be exploited in future work, to devise a detection scheme for structural defects within a pipe. We present here results from PZFlex numerical simulations, analyzed using the methodology laid out in (Alleyne & Cawley 1991). We will first introduce guided wave modes (Sec. 2), outline the time reversal stage (Sec. 3), then discuss what modes are present before and after Time Reversal has been applied for two different input waveforms (Sec. 4).

2. GUIDED WAVE MODES

Guided waves present in thin-walled cylinders, or thin shells, are very similar to Lamb waves seen in thin plates and rods. The thin shell allows for the generation of the symmetric and asymmetric wave modes, which result in Longitudinal and Flexural guided waves. In addition, there are Torsional guided waves, a propagation along the pipe of displacement in the circumferential direction, that has no analog in thin plates. In order to study these briefly, we begin with the general equation for displacement due to a guided wave mode in a thin-plate excited by a sinusoid of frequency ω is (Brekhovskikh 1960):

$$\mathbf{u}_m(\mathbf{x},t) = \mathbf{a}_m(\omega)e^{\jmath(\omega t - k_M(\omega)R(\mathbf{x}) - \phi)} \tag{1}$$

where $\mathbf{u}_m(\mathbf{x},t)$ is the 3-dimensional displacement from the m^{th} wave mode at position $\mathbf{x}$, a distance $R(\mathbf{x})$ from the wave source, and at time t. $\mathbf{a}_m(\omega)$ is that wave mode's frequency-dependent amplitude, $\omega = 2\pi f$

is the angular frequency, $k_M = \omega/\nu_m(\omega)$ is the wave number, $\nu_m(\omega)$ is the wave mode's frequency-dependent phase velocity, and ϕ is the phase term. We will ignore ϕ for the remainder of this article. Although (Brekhovskikh 1960) defines eq. 1 for (x, y, z) coordinates, we will consider cylindrical coordinates (r, θ, z).

$$\mathbf{u}_m(\mathbf{x}, t) = \begin{bmatrix} u_{m,r}(\mathbf{x}, t) \\ u_{m,\theta}(\mathbf{x}, t) \\ u_{m,z}(\mathbf{x}, t) \end{bmatrix} \tag{2}$$

Since it is difficult to measure and excite 3-axis displacement values, we will assume that the excitation and response are both restricted to one dimension, the radial axis (r). Thus, for the remainder of this paper, we will consider only the out-of-plane displacement ($u_m(\mathbf{x}, t) = u_{m,r}(\mathbf{x}, t)$). This simplification means that Torsional modes, which exhibit no displacement in the z or r dimensions, can be ignored. Their presence, however, does not change any of the results, this simplification is made in the interest of brevity.

2.1 Propagation Distance

In order to continue, we need to determine the effective propagation distance R for each guided wave mode. Longitudinal and Flexural waves are formed by the superposition of many symmetric and asymmetric modes traversing the pipe. The Longitudinal waves are axisymmetric, thus the wavefront is perpendicular to the pipe's central axis. This means that the propagation distance between a source and point of interest depends only on their separation along the central axis. Given a source at point $\mathbf{x}_0 = (0, 0, r)$, the displacement at point $\mathbf{x} = (r, \theta, z)$ in cylindrical coordinates is

$$R_L(\mathbf{x}) = z \tag{3}$$

Flexural waves, however, are non axisymmetric, so their propagation distance is more difficult to compute analytically, so we simply write: $R_F(\mathbf{x})$.

2.2 Amplitude Function

From (Li & Rose 2000), we know that the amplitude function for Longitudinal wave modes, if we ignore attenuation, is independent of distance z. Furthermore, a property of axisymmetry is that their displacement (in cylindrical coordinates) is also independent of angle θ (Gazis 1959). Thus, for these modes we can simply write $a_L(r, \omega)$. Flexural wave modes, however, have an amplitude function that is wholly dependent on position $\mathbf{x}$. Thus, we write $a_F(\mathbf{x}, \omega)$.

2.3 Displacement Equation

There are an infinite number of wave modes (for Longitudinal, Torsional and Flexural), but each Flexural mode also has an infinite number of circumferential orders, making them doubly infinite, each mode-order pair resulting in it's own amplitude function $a_F^M(\mathbf{x}, \omega)$, wavenumber $k_F^M(\omega)$, and propagation distance $R_F^M(\omega)$. If we consider the aggregate superposition of every mode excited, we have the channel response:

$$u(\mathbf{x}, t) = \underbrace{\sum_{L=0}^{\infty} a_L(r, \omega) e^{\jmath(\omega t - k_L(\omega) z)}}_{\text{Longitudinal}} + \underbrace{\sum_{F=0}^{\infty} \sum_{M=0}^{\infty} a_F^M(\mathbf{x}, \omega) e^{\jmath\left(\omega t - k_F^M(\omega) R_F^M(\mathbf{x})\right)}}_{\text{Flexural}} \tag{4}$$

In order to continue, we now take the Fourier transform along the time domain for angular frequency at some sample point ω_q.

$$U(\mathbf{x},\omega_q) = \int_{-\infty}^{\infty}\left\{\sum_{L=0}^{\infty} a_L(r,\omega)e^{\jmath(\omega t - k_L(\omega)z)} + \sum_{F=0}^{\infty}\sum_{M=0}^{\infty} a_F^M(\mathbf{x},\omega)e^{\jmath\left(\omega t - k_F^M(\omega)R_F^M(\mathbf{x})\right)}\right\} e^{-\jmath\omega_q t}dt \quad (5)$$

$$= \left\{\sum_{L=0}^{\infty} a_L(r,\omega)e^{-\jmath k_L(\omega)z} + \sum_{F=0}^{\infty}\sum_{M=0}^{\infty} a_F^M(\mathbf{x},\omega)e^{-\jmath k_F^M(\omega)R_F^M(\mathbf{x})}\right\}\delta(\omega-\omega_q) \quad (6)$$

$$= \left\{\sum_{L=0}^{\infty} a_L(r,\omega_q)e^{-\jmath k_L(\omega_q)z} + \sum_{F=0}^{\infty}\sum_{M=0}^{\infty} a_F^M(\mathbf{x},\omega)e^{-\jmath k_F^M(\omega_q)R_F(\mathbf{x})}\right\}\delta(\omega-\omega_q) \quad (7)$$

where $\delta(x)$ is the indicator (or dirac) function. We call this expression the **Channel Transfer Function** at that frequency. Thus, if we consider a broadband input signal $S(\omega)$, as a strain at some point, we can expect the output at any position $\mathbf{x}$ down the pipe to be:

$$Y(\mathbf{x},\omega_q) = S(\omega_q)U(\mathbf{x},\omega_q) \quad (8)$$

2.4 2-D FFT Analysis

We will use the 2-D FFT of the incident wave at a series of transducers in order to analyze the dispersion curve for our pipe. In order to take the FFT of (7) along the z axis, we must first make two fundamental assumptions. 1) That the z-extent of the region in question is small enough to ignore attenuation and variation of the Flexural mode amplitude function. This leads to the approximations $a_L(r,\omega) \approx a_L(r,z_0,\omega)$ and $a_F^M(\mathbf{x},\omega) \approx a_F^M(r,\theta,z_0,\omega)$ for some z_0 inside the region. 2) That the flexural propagation distance $R_F^M(\mathbf{x})$ is linear in z $\left(R_F^M(\mathbf{x}) = b_F^M(r,\theta)z + c_F^M(r,\theta)\right)$. Under these assumptions:

$$U(k,\omega_q) = \left[\sum_{L=0}^{\infty} a_L(r,z_0,\omega)\delta\left(k-k_L(\omega_q)\right)\right. \quad (9)$$

$$\left. + \sum_{F=0}^{\infty}\sum_{M=0}^{\infty} a_F^M(r,\theta,z_0,\omega)e^{-\jmath k_F^M(\omega_q)c_F^M(r,\theta)}\delta\left(k-k_F^M(\omega_q)b_F^M(r,\theta)\right)\right]\delta(\omega-\omega_q)$$

If we plot this 2-D image, using a grayscale for intensity, then we will see each wave mode trace out a single line along the coordinates $(\omega_q, k_L(\omega_q))$ or $(\omega_q, k_F(\omega_q)b_F^M(r,\theta))$ $\forall\omega_q$. This series of mode-curves is seen in the theoretical dispersion curve (Figure 1) and the computed dispersion curves (Figures 4 and 7).

3. TIME REVERSAL PROCESSING

Time Reversal is based on the assumptions of channel reciprocity and stationarity. In other words, ignoring noise, if we have transducers A and B, then if we transmit some pulse from A to B, we will receive the same result as if we transmit that pulse from B to A (reciprocity), and if we repeat that transmission at any later time, the results will be the same. In time reversal, we perform a three-stage process.

- *Conventional Probing* A pulse is transmitted from A, through the channel, to B
- *Time Reversal Processing* The received signal is time-reversed and energy-normalized
- *Time Reversal Probing* The new TR signal is transmitted from B, back through the channel, to A

So, if we define $\mathbf{x}_B$ as the position of antenna B and $\mathbf{x}_0 = (0, 0, r)$ as the position of antenna A, then the received signal due to a real input $\mathbf{S}(\omega)$ at A is:

$$Y(\omega_q) = S(\omega_q)U(\mathbf{x}_B, \omega_q) \tag{10}$$

And, if this is time reversed (negation of the angular frequency term in the frequency domain), then the probing signal becomes

$$S_{TR}(\omega_q) = kY(-\omega_q) = kS(-\omega_q)U(\mathbf{x}_B, -\omega_q) \tag{11}$$

where k is the energy normalization term, given by:

$$k = \sqrt{\frac{\sum_{q=0}^{Q-1} |S(\omega_q)|^2}{\sum_{q=0}^{Q-1} |S(\omega_q)U(\mathbf{x}_B, \omega_q)|^2}} \tag{12}$$

We note that the signal $S(\omega)$ has a real-valued Fourier Transform, thus $S(-\omega) = S^*(\omega)$. The received signal, back at antenna A is

$$\begin{aligned} Y_{TR}(\omega_q) &= S_{TR}(\omega_q)U(\mathbf{x}_B, \omega_q) && (13)\\ &= kY(-\omega_q)U(\mathbf{x}_B, \omega_q) && (14)\\ &= kS^*(\omega_q)U(\mathbf{x}_B, -\omega_q)U(\mathbf{x}_B, \omega_q) && (15) \end{aligned}$$

We make the assumption that phase speed is even symmetric with respect to ω, thus $\nu_m(\omega_q) = \nu_m(-\omega_q)$. This leads to the relationship

$$k_M(-\omega_q) = -k_M(\omega_q),\ k_F^M(-\omega_q) = -k_F^M(\omega_q) \tag{16}$$

The same even symmetry assumption is made for the real gain terms $a_L(r, \omega)$ and $a_F^M(\mathbf{x}, \omega)$. Thus, we have the product

$$\begin{aligned} U(\mathbf{x}_B, -\omega_q)U(\mathbf{x}_B, \omega_q) &= \left[\sum_{L=0}^{\infty} a_L(r,\omega)e^{\jmath k_L(\omega_q)z} + \sum_{F=0}^{\infty}\sum_{M=0}^{\infty} a_F^M(\mathbf{x},\omega_q)e^{\jmath k_F^M(\omega_q)R_F^M(\mathbf{x})}\right] \\ &\quad * \left[\sum_{L=0}^{\infty} a_L(r,\omega)e^{-\jmath k_L(\omega_q)z} + \sum_{F=0}^{\infty}\sum_{M=0}^{\infty} a_F^M(\mathbf{x},\omega_q)e^{-\jmath k_F^M(\omega_q)R_F^M(\mathbf{x})}\right] && (17)\\ &= \left|\sum_{L=0}^{\infty} a_L(r,\omega)e^{-\jmath k_L(\omega_q)z} + \sum_{F=0}^{\infty}\sum_{M=0}^{\infty} a_F^M(\mathbf{x},\omega_q)e^{-\jmath k_F^M(\omega_q)R_F^M(\mathbf{x})}\right|^2 && (18) \end{aligned}$$

Thus, (15) becomes:

$$Y_{TR}(\omega_q) = kS^*(\omega_q)\,|U(\mathbf{x}_B, \omega_q)|^2 \tag{19}$$

We can see from (19) that the received signal has the same phase-profile as the transmitted signal. Thus, the channel now behaves like a linear phase filter, with no dispersion effects. This is the cause of Time Reversal's time compression (Ing & Fink 1998). Furthermore, the $|U(\mathbf{x}_B, \omega_q)|^2$ term acts like an adaptive power allocation scheme, concentrating power in those frequency bands that are passed through the channel more efficiently, and attenuating those bands which do not effectively transmit energy.

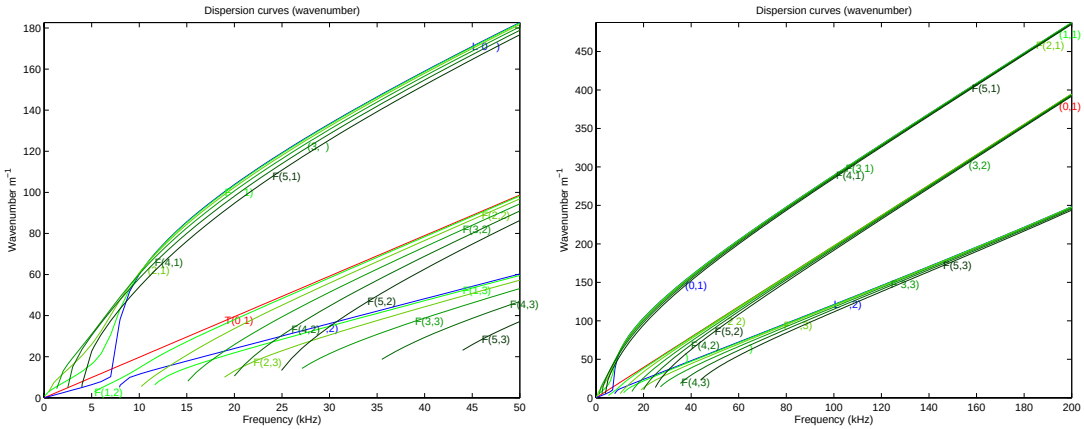

Figure 1: Dispersion curve for the pipe modeled, showing wavenumber vs. frequency for Longitudinal, Torsional, and first-order Flexural modes for f=0-50kHz (left) and f=0-200kHz (right).

4. NUMERICAL SIMULATIONS

We used the commercial PZFLex software package on a Dell Inspiron running 64-bit Fedora 9 to run the numerical simulations. The pipe modeled has outside diameter .22m, inside diameter .204m, and length 6m. We placed the transmitter at x=.5m from the end of the pipe, and measured the incident wave down the pipe at 400 sample points from x=3m to x=5m, with a spacing of 5mm between the sample points. We model the input as a voltage across the terminals of a PZT5a patch, with dimensions 2.8mm x 0.7mm. The pipe has a hole, 11mm wide, extending 50mm from x=2.5m to x=3m. In order to verify that Time Reversal will indeed be beneficial for detection of structural defects, it was necessary to test performance on a defected pipe, as the boundary conditions and mode conversions made analysis unclear. We consider this single set of tests as verification that TR focusing is a valid procedure in both structurally clean and damaged pipes.

Inputs are modeled as a compressive strain in the z direction, and the received signal is the z-axis displacement of a particle at the receiver position.

Using the freely available PCDISP (Seco, Martín, Jiménez, Pons, Calderón & Ceres 2002) package for MATLAB, we computed the expected dispersion curves for guided waves within this pipe. We computed the Longitudinal, Torsional, and first 5 circumferential orders of Flexural modes, and show the plot of wavenumber vs. frequency in figure 1 for two different cutoff frequencies. In the absence of dispersion, each mode's propagation velocity ν is independent of frequency, resulting in a wavenumber that is linear in frequency (recall that $k = \omega/\nu$). Thus, any non-linearity of the traces in the dispersion curves is an artifact of dispersion.

4.1 Narrowband Gaussian Pulse Excitation

We first use a relatively narrowband Gaussian pulse, centered at $f_c = 100kHz$, with a two-sided -6dB bandwidth of $BW = 50kHz$. Figure 2 shows the probing signal (left) and received response at x=5m (right). It is evidently clear that, even for this relatively narrow-band system, there is a large contribution from delayed arrivals of the signal.

We then time-reverse and energy-normalize the received signal before using it as the TR excitation signal. Figure 3 shows the TR probing signal (left) and received response at x=5m (right). Even in this narrowband system, we can see the significant amount of time compression achieved by Time Reversal. Furthermore the maximum amplitude of the received signal has increased from roughly .2μm to .6μm.

In order to analyze the wave modes present, we take the received signal, sampled at 400 points with

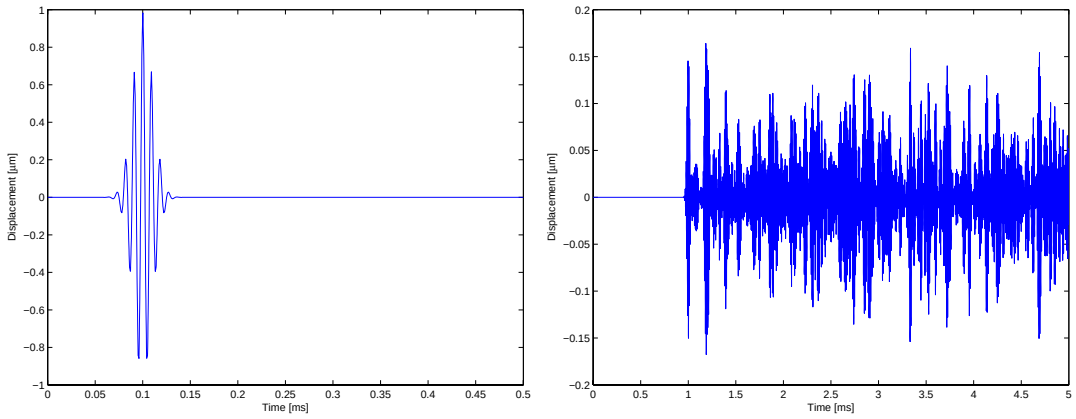

Figure 2: Probing signal (left) and response (right) for the narrowband Gaussian excitation, centered at 100kHz.

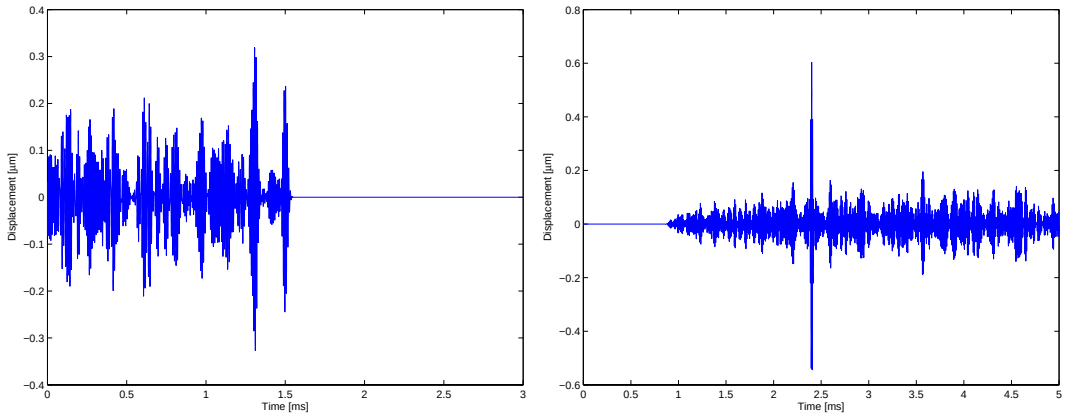

Figure 3: TR probing signal (left) and response (right) for the narrowband Gaussian excitation, centered at 100kHz.

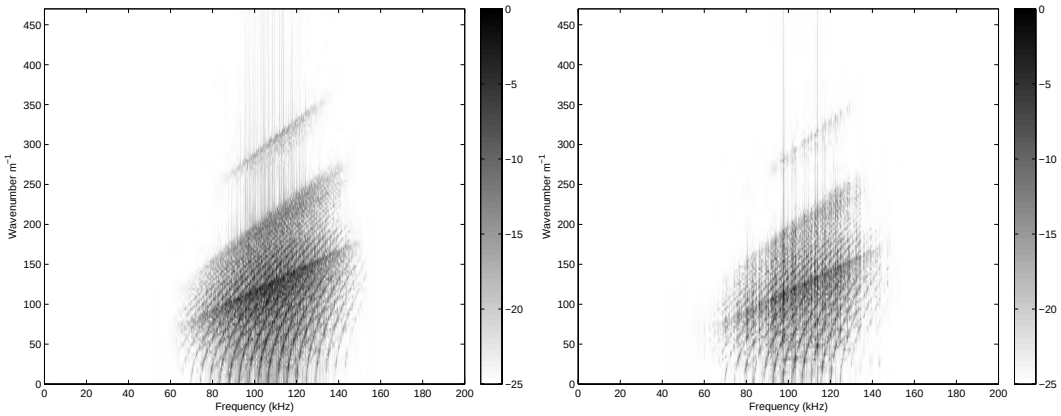

Figure 4: Calculated dispersion curves (plotted in log scale) for the conventional (left) and TR (right) cases.

a spacing of $\delta_x = 5mm$, for a period of .5ms with a sampling frequency of roughly $f_s = 6MHz$. In figure 4, we show the 2-D FFT of this received signal both for the standard (left) and the Time Reversal (right) probing signals. Compare the results to figure 1. The results in figure 4 show many more modes converging to similar wavenumber paths as those shown in figure 1. This is because the theoretical curves were only plotted for the first 5 circumferential orders of the Flexural waves, while an infinite number of circumferential orders exist in the pipe.

Between the two dispersion curves, it is evident that there are some wave-modes present in the forward transmission that are not replicated in the TR transmission, or are present with a lower amplitude. This is due to the channel matching property of Time Reversal. In utilizing the time-reversed received signal from the forward case, the TR probing signal adaptively allocates power to those wave-modes which exhibit more efficient transmission of power. Most significantly, we can see that the 1st-order modes (see Figure 1, L(0,1) and F(M,1)) are suppressed in the TR case. Whether these variations in mode amplitude are due to well known dependence on the characteristics of the source loading (Li & Rose 2000), or as a result of the defect modeled in our simulation is unclear.

4.2 Wideband Sinc Pulse Excitation

Next, we show the results for a wideband sinc pulse with cutoff frequency of $f_{cutoff} = 200kHz$. Figure 5 shows the probing signal (left) and received response at x=5m (right). It is clear from the result that the effects of dispersion and mode superposition are amplified in this case, over the narrowband scenario. That is to be expected, as the sinc is exciting a much larger bandwidth, resulting in higher modes and more dispersion.

We then time-reverse and energy-normalize the received signal before using it as the TR excitation signal. Figure 6 shows the TR probing signal (left) and received response at x=5m (right). As before, we again see a significant time compression, with the maximum received amplitude increasing from roughly .1μm to .55μm, a 7.4dB increase.

Taking the 2-D FFT, we have the dispersion curves shown in figure 7. After Time Reversal, we can see a reduction in the higher order flexural modes (seen in the bottom-right and center-right portions of the plot). Figure 8 shows the spectrum of the originally transmitted sinc waveform(solid line), as well as the TR waveform used in step 3(dotted line). In this scenario, the band from 150kHz-200kHz is not as efficient as the lower frequency bands, so less power is transmitted there, resulting in a lower amplitude for those high-order wave modes.

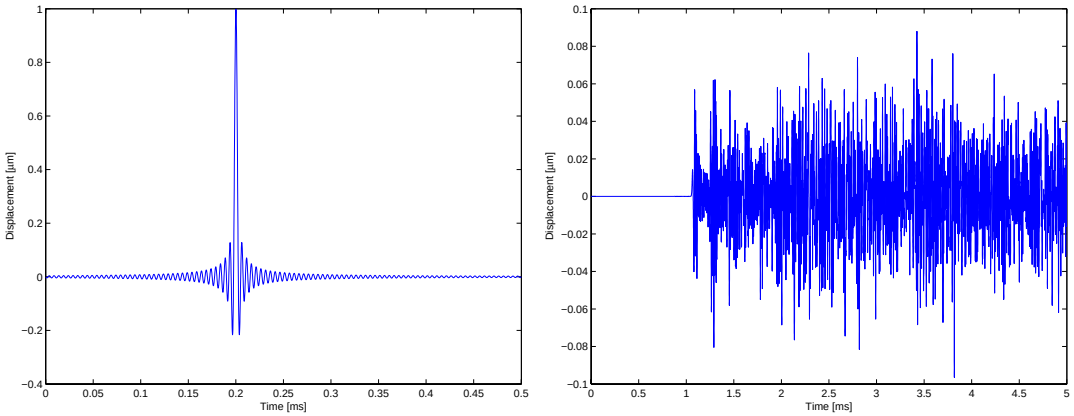

Figure 5: Probing signal (left) and response (right) for the wideband Sinc excitation, with cutoff of 200kHz.

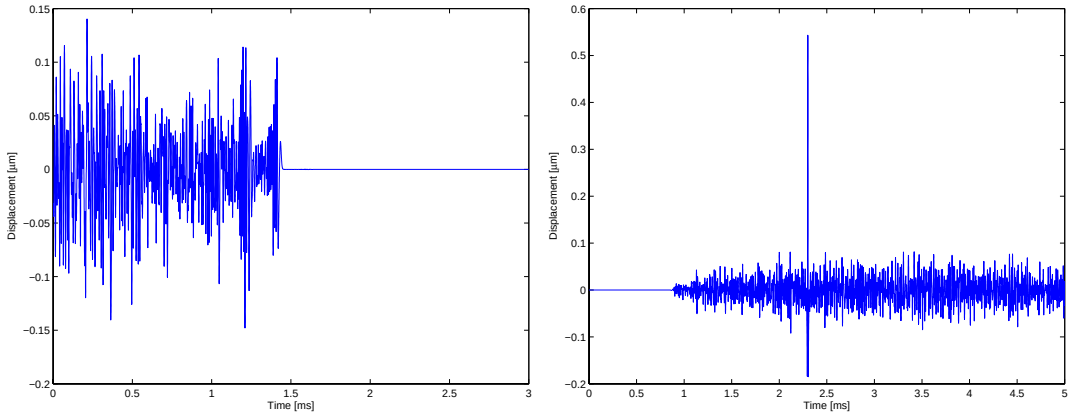

Figure 6: TR probing signal (left) and response (right) for the wideband Sinc excitation, with cutoff at 200kHz.

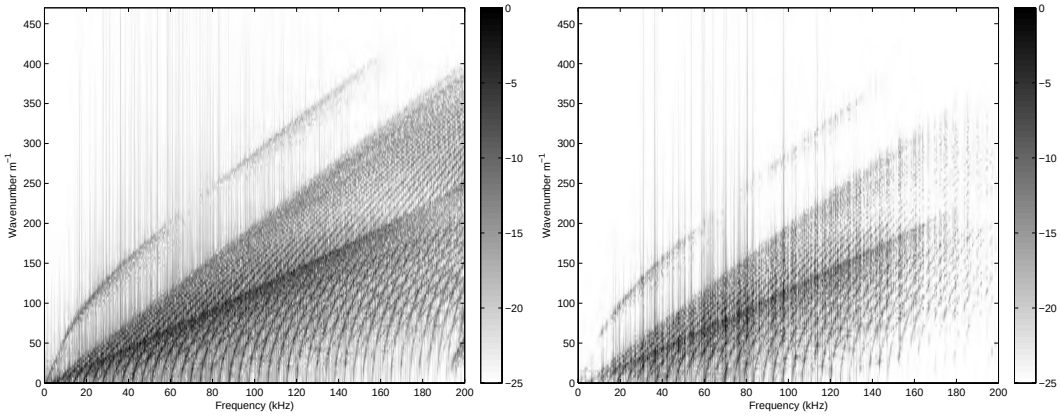

Figure 7: Calculated dispersion curves (plotted in log scale) for the conventional (left) and TR (right) cases.

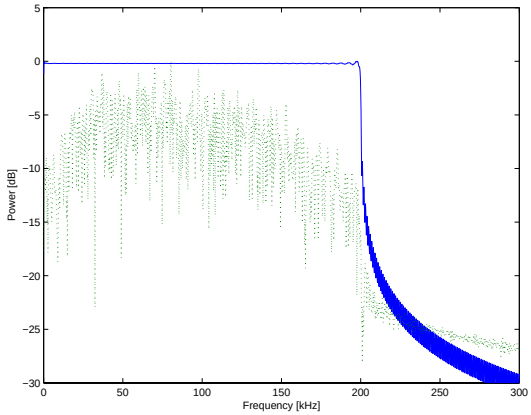

Figure 8: Spectrum of Sinc (solid) and TR (dotted) probing signals.

5. CONCLUSION

We have shown here a derivation for the effect of Time Reversal on the received signal when exciting guided wave modes within a cylindrical pipe. Through numerical simulations, we have confirmed the time compression effect of Time Reversal with guided waves, as well as the selective excitation of those wave modes which most effectively transmit energy through the pipe. This matches the results reported by Ing and Fink (Ing & Fink 1998) for thin plates. This is a promising preliminary study, and will guide our future work in devising a Time Reversal based detector for structural faults within pipes. Specifically, it is necessary to analyze the differences in TR focusing for clean pipes and pipes with various amounts of damage, in order to determine how best to enhance the effects of damage.

6. ACKNOWLEDGMENTS

National Energy Technology Laboratory (NETL) is the funding source for this effort with Cost Share being provided by Carnegie Mellon University (CMU). Concurrent Technologies Corporation (CTC) is funded under a cooperative agreement with NETL. CMU is funded under a Subcontract Agreement with CTC. Nicholas O'Donoughue is supported by National Defense Science and Engineering Graduate Fellowship, sponsored by the Army Research Office.

REFERENCES

Alleyne, D. N., & Cawley, P. A. (1991), "A two-dimensional Fourier transform method for the measurement of propagating multi-mode signals," *J. Acoust. Soc. Amer.*, 89, 1159–1168.

Brekhovskikh, L. M. (1960), *Waves in Layered Media* Academic.

Fink, M. (1992), "Time Reversal of Ultrasonic Fields, I: Basic Principles," *IEEE Trans. on Ultrasonics, Ferroelectrics, and Frequency Control*, 39, 555–566.

Gazis, D. C. (1959), "Three-Dimensional Investigation of the Propagation of Waves in Hollow Circular Cylinders. I. Analytical Foundation," *J. Acoust. Soc. Am.*, 31(5), 568–573.

Ing, R. K., & Fink, M. (1998), "Time-Reversed Lamb Waves," *IEEE Trans. on Ultrasonics, Ferroelectrics, and Frequency Control*, 45(4), 1032–1043.

Jin, Y., & Moura, J. M. F. (2009), "Time-Reversal Detection Using Antenna Arrays," *IEEE Trans. on Signal Processing*, 57(4), 1396–1414.

Li, J., & Rose, J. L. (2000), "Excitation and propagation of non-axisymmetric guided waves in a hollow cylinder," *J. Acoust. Soc. Am.*, 109(2), 457–464.

Moura, J. M. F., & Jin, Y. (2007), "Detection by Time Reversal: Single Antenna," *IEEE Trans. on Signal Processing*, 55(1), 187–201.

Moura, J. M. F., & Jin, Y. (2008), "Time Reversal Imaging by Adaptive Interference Canceling," *IEEE Trans. on Signal Processing*, 56(1), 233–247.

Prada, C., & Fink, M. (1998), "Separation of interfering acoustic scattered signals using the invariants of the time-reversal operator. Application to Lamb waves characterization.," *J. Acoustic. Soc. Am.*, 104(1), 801–807.

Seco, F., Martín, J. M., Jiménez, A., Pons, J. L., Calderón, L., & Ceres, R. (2002), PCDISP: A Tool for the simulation of wave propagation in cylindrical waveguides,, in *Proc. 9th Int'l Congress on Sound and Vibration*, pp. 23–29.